Numerical simulations of Kadomtsev-Petviashvili soliton interactions

E. Infeld, A. Senatorski, and A. A. Skorupski
Soltan Institute for Nuclear Studies, Hoża 69, 00-681 Warsaw, Poland
(Received 19 August 1994; revised manuscript received 7 November 1994)

The Kadomtsev-Petviashvili equation generalizes that of Korteweg and de Vries to two space dimensions and arises in various weakly dispersive media. Two very different species of soliton solutions are known for one variant, KPI. The first species to be discovered are line solitons, the second are two dimensional lumps. This paper describes numerical simulations, consistent with all constraints of the equation, in which very distorted line solitons break up into smaller line solitons and arrays of lumps. The arrays can interact with one another. In some cases, aspects of the results of the simulations can be understood in the light of specially constructed exact solutions. Simulations in which initial conditions fail to satisfy the constraints of the equation are also described.

PACS number(s): 47.20.Ky, 52.35.Sb, 52.35.Py

I. INTRODUCTION

The Kadomtsev-Petviashvili equation [1]

$$(n_t+6nn_x+n_{xxx})_x+3\varepsilon n_{yy}=0, \quad \varepsilon=\pm 1 \tag{1.1}$$

is of both mathematical and physical interest. In this form, it is not an evolution equation. (However, it is when written without the overall x differentiation but with a ∂_x^{-1} operator in front of the last term. This choice is discussed in [2].) For $\varepsilon=-1$ the equation is designated KPI and has two distinct and different kinds of soliton solutions. The first are line solitons and several of these can propagate at acute angles to each other, each with a constant velocity $\mathbf{v}_i$ when they are well separated. The amplitudes and speeds are all different. In mathematical terms, the building blocks of these solitons are exponentials. The second kind are lumps bounded in all directions [3]. They collide without distortion or change of phase. Again, no two amplitudes are equal. The lumps are unusual in that they are described mathematically by ratios of polynomials rather than the more common exponentials. For more information on the two classes of solitons see Ref. [4]. Similar behavior is found for another two-dimensional (2D) equation, Davey-Stewartson II [5,6].

Arrays of lumps have recently been found as exact solutions [7,8]. It has in fact been shown that these arrays can be represented by sums of lump solitons [7], even though the former are given in terms of trigonometric and hyperbolic functions. Recently, exact solutions corresponding to cohabiting line solitons and arrays of lumps have also been found [9]. In this paper, when trying to understand the results of our numerical simulations, we will extend some of this work and find exact solutions that fit the results quantitatively.

The present work mainly reports results of numerical simulations and such exact solutions as will elucidate some aspects of these simulations. However, quite a lot of general work on KPI has been done to date and a few results should be mentioned here.

The Riemann-Hilbert problem was first established by Manakov [10]. The spectral significance of the lumps was elucidated in Refs. [11] and [12], where Manakov's study was completed and it was shown that the spectral analysis of the Lax pair associated with KPI leads to a nonlocal Riemann-Hilbert problem for some eigenfunction $\mu(x,y,t,k)$. (The Lax pair was first found in [13].) This eigenfunction satisfies a Fredholm integral equation and hence can have homogeneous solutions at $k=k_j$. These eigenvalues give rise to lumps. Thus, lumps in two dimensions are generic and the analogs of solitons in one dimension. Arbitrary decaying initial data will decompose into a number of lumps. This is an analog of the fact that arbitrary compact initial data of an integrable equation in one space dimension will decompose into a number of solitons.

In this paper, we will take distorted *line* solitons as our initial conditions and the above general results will not apply. Some incomplete theoretical results, however, do suggest that line solitons will tend to break up into new line solitons and lumps [14]. As already mentioned, some special exact solutions found recently confirm this behavior, believed to be general [9].

Recently, the present authors looked at a simulation in which a "wiggled" line soliton constituted the initial condition. The "wavelength" of the distortion corresponded to the maximum growth rate of a linear perturbation (though we are not dealing with linear perturbation here). The distorted line soliton decomposed into lumps and a small, residual line soliton [15]. Almost simultaneously, an exact solution exhibiting *somewhat* similar behavior appeared in the English language literature [9].

In this paper, we will present those numerical simulations that are far from, and not representable by, any simple exact solutions. However, in some cases these latter solutions will help us understand some aspects of the simulations.

Understanding a problem as complex as the decay and interaction of different kinds of solitons should begin with some simplification. Here we will assume all asymptotic velocities to be along x. This still seems to include all the important physics.

Before we proceed, a few words about the physical derivation of both KPI and KPII would seem to be in order. In deriving (1.1) in a wide range of physical contexts, it is assumed that a soliton or wave is either moving along x or else propagating at a very acute angle to the x axis, always from left to right. Changes in y are taken to be much slower than along the line of motion. Furthermore, the velocity of soliton propagation differs only slightly from that of sound. The equation is in all cases nondimensional, the unit of velocity being the velocity of sound, e.g., $(gh)^{1/2}$ for shallow water waves, $(K_B T_e/m_i)^{1/2}$ in a two-component, electron-ion plasma. In all cases considered, a whole host of phenomena occur at velocities slightly in excess of these sonar values. It is amazing just how much physics survives all the approximations involved in deriving (1.1) when considering weakly dispersive media.

An extensive derivation of (1.1), including an ordering of small parameters, is given in Chap. 5 of Ref. [4]. Equation (1.1) is integrable by inverse scattering [10,11] and the simplest way of convincing oneself of this is to perform a Painlevé analysis [16].

The simplest soliton solution to (1.1) is, regardless of ε,

$$n(x,t)=2p^2\mathrm{sech}^2[p(x-4p^2t)] , \tag{1.2}$$

where p is a parameter and n is the excess of the density over its average value n_0, always positive for this solution, but not for others we will encounter later on. The soliton (1.2) was investigated for stability with respect to two-dimensional perturbations [17,18]. Theory indicates stability for $\varepsilon=1$ (KPII), instability for $\varepsilon=-1$ (KPI). Numerical simulations have so far confirmed these statements [15,18]. In these references the *phase* was perturbed by adding a term proportional to $\cos(k_y y)$. The soliton was seen to wiggle periodically, but otherwise remain intact for KPII, but to break up as described above for KPI. Here we will address KPI only.

II. NUMERICAL RESULTS

Our calculations were performed on the HP-Apollo model 720 work station. The numerical algorithm used for calculating the time evolution was the leapfrog algorithm when (1.1) was integrated over x. The essence of this algorithm consists of replacing the time derivative by its symmetric difference approximation, $[n(t+\Delta t)-n(t-\Delta t)]/2\Delta t$. The fast Fourier transform method was used to calculate x and y derivatives. The scheme was shown to be numerically stable for sufficiently short time steps (see Appendix for details).

As an introductory exercise, we compared the results of a dynamical simulation with the exact solution corresponding to one lump [3]:

$$n_0(x,y,t)=\frac{4\nu[1-\nu(x-3\nu t)^2+\nu^2y^2]}{[1+\nu(x-3\nu t)^2+\nu^2y^2]^2} . \tag{2.1}$$

With initial condition for the dynamical simulation

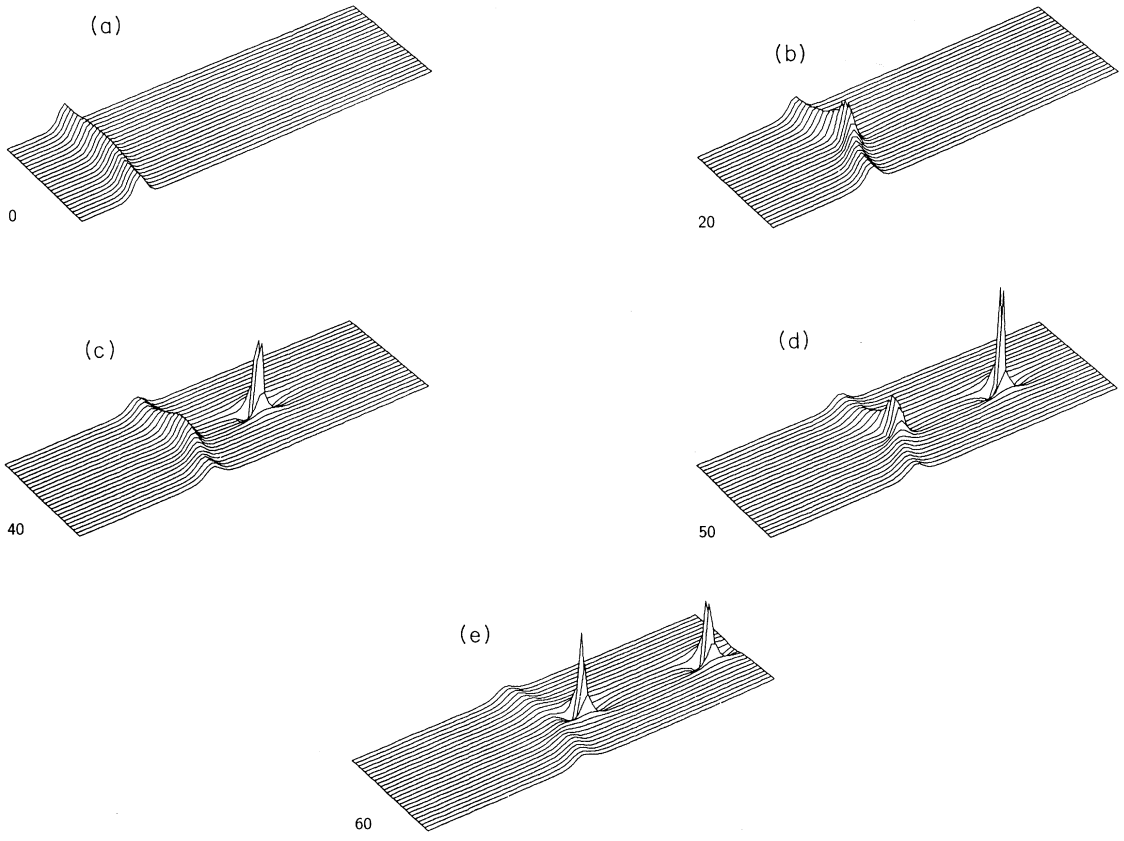

FIG. 1. Decay of a distorted line soliton with $\delta=0.04$.

$n = n_0(x,y,0)$, we maintained very good accuracy during the entire simulation.

A second check on the accuracy was a comparison of the products of disintegration of a slightly wiggled line soliton. (Numerical noise on its own was not sufficient to destabilize it on a reasonable time scale.) These products emerged after a while and were of the type of (2.1). Here agreement was also very good and can be seen in Ref. [15]. (Unfortunately, reduction of Fig. 2 in Ref. [15] is not the same as that of Fig. 1. It should be further reduced by $\frac{2}{3}$. When this is done, an extremely good fit is obtained.)

We now present the main results of this work, namely the decay of the soliton (1.2) when wiggled such that the phase at $t=0$ becomes

$$p(x-x_0)+\delta\cos(k_y y)\ . \tag{2.2}$$

The Kadomtsev-Petviashvili equation (1.1) is peculiar in that the initial condition must fulfill an infinite set of constraints if the solution is to remain localized in x [19]. (However we only need worry about these constraints at $t=0$.) The first is obtained by integrating (1.1) over x,

$$\partial_{yy}\int_{-\infty}^{\infty} n\,dx = 0\ , \tag{2.3}$$

and the others are more complicated. Obviously, bending as in (2.2) will satisfy these constraints. On the other hand, the most commonly used perturbation in problems of this type,

$$n = [1+\delta\cos(k_y y)]n_0\ , \tag{2.4}$$

would violate them. However, we will use the above as an initial condition, just to see what happens when the constraints are not satisfied, in Sec IV.

In Ref. [15] the phase alteration amplitude δ in (2.2) was taken to be small and k_y corresponded to the maximum growth rate of a linear perturbation, known to be $2p^2/3$ [17]. A single array of lumps, plus a small residual line soliton, were formed. Due to the smallness of δ ($=0.016$) this was somewhat similar to an exact solution found around the same time [9] (and of course not known to us). To see the similarity, compare Figs. 1 of Refs. [9] and [15].

The rationale of the present paper is to present the results of numerical simulations far from the simple exact solutions given in Ref. [9] or indeed obtainable in any way (by simple we mean presentable as sums rather than integrals). Thus here the δ in (2.2) will be taken to be noticeable and large (0.04 and 0.4, respectively) and distortions of the line soliton finite. However, an exact solution will be seen to elucidate some aspects of our results (Sec. III).

In Fig. 1, distortion of the line soliton is small but noticeable ($\delta=0.04$). The initial bending of the soliton induces a corresponding variation of the height. The line soliton is next seen to break up into a much smaller line soliton and two arrays (due to the assumed periodicity in y, this drawing is to be imagined repeated in the y direc-

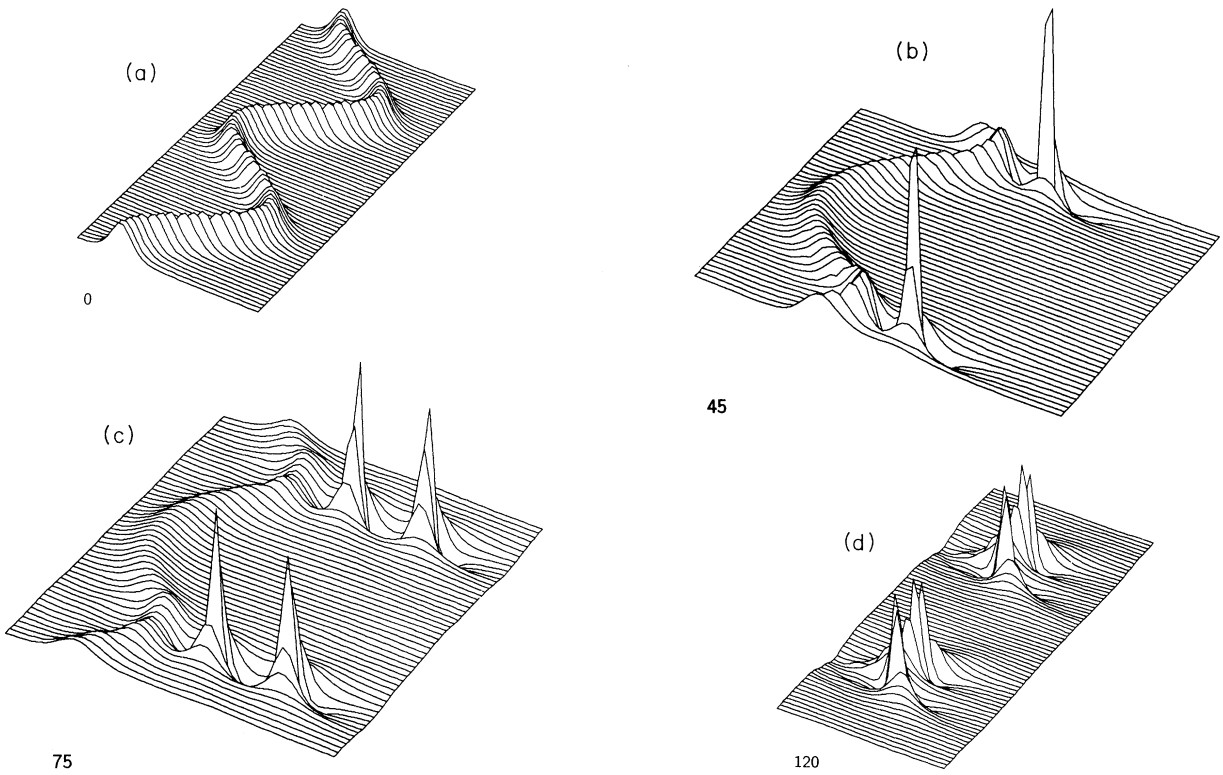

FIG. 2. Decay of a strongly distorted line soliton, $\delta=0.4$. The fourth and following frames exclude the residual distorted line soliton. Frames (f) through (j) correspond to the enlarged center of (e).

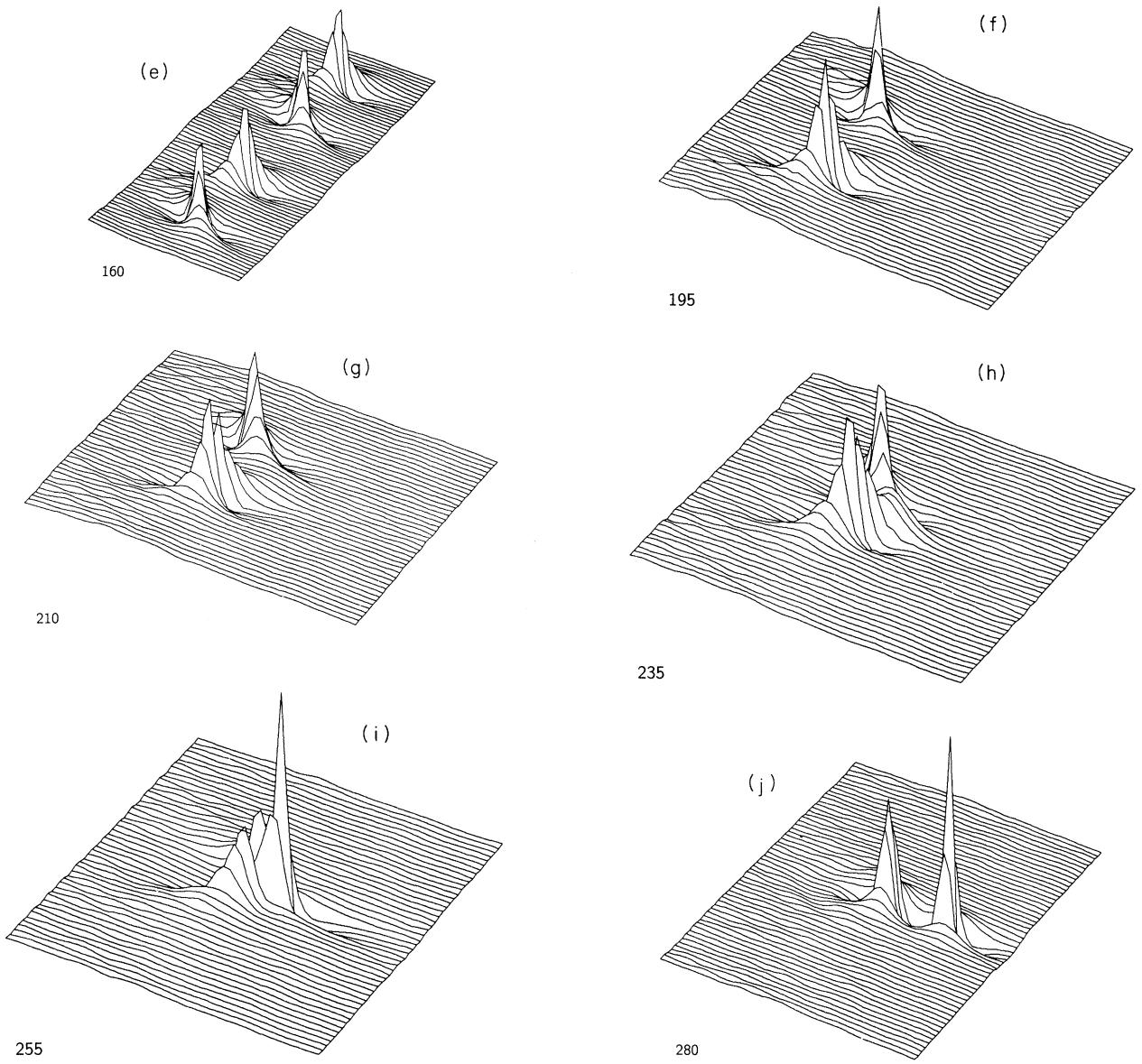

FIG. 2 *(Continued).*

tion *ad infinitum).* When δ was just 0.016, as in Ref. [15], only one array of lumps was produced.

In Fig. 2, the distortion of the initial line soliton is large ($\delta=0.4$). Initially, two arrays of lumps were produced. Those on the left were larger and so subsequently caught up with the lumps on the right. Interestingly, the resulting tandem then shifted in y by half a wavelength of the array and then separated. This took us by surprise, but will become clearer in Sec. III. After a while, a third array emerged (outside the frame).

In a fourth simulation (counting that of Ref. [15]), not shown here, we collided an array of lumps with a line soliton. The array emerged unaltered but once again shifted by half a wavelength in the y direction.

Thus the $\lambda/2$ perpendicular shift (not to be confused with phase shifts in x) seems to be a general phenomenon, though as far as we can see unnoticed so far in the otherwise extensive literature on KPI.

In Sec. III we will try to shed some theoretical light on all the above phenomena.

III. THEORETICAL INTERPRETATION

When the line soliton was distorted very weakly (δ small), one array of lumps was produced on the time scale of the simulation [15]. However, when δ was somewhat larger, two arrays emerged. A somewhat qualitative explanation of this would be as follows.

For δ very small, a feasible approximation to our initial condition is the sum of a line soliton and an initially very small array of lumps with "wave number" k_y. These two entities will separate after a while and at the same time

the lumps will grow (the value of k_y was chosen to correspond to the maximum growth rate of a linear perturbation and this can be shown to be equal to the maximum growth rate of an infinitesimal array of lumps on top of a line soliton [9]).

When δ is increased, the one periodic mode approximation is insufficient, and a second $2k_y$ array must be introduced to approximate the initial condition. This value is beyond the range of instability and the second component will not grow. However, due to nonlinear interaction, a third array such that $k_{y3}=2k_y-k_y=k_y$ will arise. Therefore, after a while, a second array of lumps with identical y spacing as the first will emerge.

As δ is further increased, so will the number of arrays increase, all with the same k_y, as no other difference mk_y-nk_y gives an "unstable" wave number. Indeed, for $\delta=0.4$ we saw a third array of lumps in the making.

This simple picture follows from our choice of $k_y=2p^2/3$ (while the maximum unstable wave number k_y is p^2). Considerably smaller values of k_y would admit new unstable $(m-n)k_y$ values and the family of emerging lumps could be more complicated.

Figure 2 shows the decay of a strongly distorted line soliton. Now increase of δ has opened the door to new phenomena: array collision and subsequent phase shifts in y. Although no simple exact solution can even approximate our simulation as described here, we can construct an exact solution corresponding to a faster array of lumps catching up with a slower array. Assuming that some aspects of our simulation can be isolated from the general context, this exact solution might confirm the possibility of a shift in y, as observed.

To find simple solutions to (1.1) we substitute

$$n=2(\ln\phi)_{xx} \ . \tag{3.1}$$

Following the method outlined in Chap. 5 of Ref. [4], a solution for ϕ that may be new (e.g., not to be found explicitly in [4], [9], or [20]) can be found from a 4×4 determinant in the form

$$\begin{aligned}
\phi=&1+\exp\{-2[(p_1+p_2)x-(\omega_1+\omega_2)t]\}\\
&+\frac{2\cos(k_y y)}{p_1}\left[\frac{A}{|CD|}\right]^{1/2}\{s+\exp[-2(p_2x-\omega_2t)]\}\exp[-(p_1x-\omega_1t)]\\
&+\frac{2\cos(k_y y)}{p_2}\left[\frac{B}{|CD|}\right]^{1/2}\{s+\exp[-2(p_1x-\omega_1t)]\}\exp[-(p_2x-\omega_2t)]\\
&+\frac{2\exp\{-[(p_1+p_2)x-(\omega_1+\omega_2)t]\}}{p_1p_2|CD|\sqrt{AB}}[C+D\cos(2k_y y)]\\
&+\frac{1}{|CD|}\{\exp[-2(p_1x-\omega_1t)]+\exp[-2(p_2x-\omega_2t)]\} \ ,
\end{aligned}$$

$$A=\frac{k_y^2}{p_1^2(k_y^2-p_1^4)}\geq0, \quad C=\frac{k_y^2-p_1^2p_2^2\left[\dfrac{p_1-p_2}{p_1+p_2}\right]^2}{k_y^2-p_1^2p_2^2} \ ,$$

$$B=\frac{k_y^2}{p_2^2(k_y^2-p_2^4)}\geq0, \quad D=\frac{k_y^2-p_1^2p_2^2}{k_y^2-p_1^2p_2^2\left[\dfrac{p_1+p_2}{p_1-p_2}\right]^2} \ ,$$

$$\omega_i=p_i^3+3k_y^2/p_i, \quad s=\frac{CD}{|CD|} \ . \tag{3.2}$$

When interpreting this solution it is useful to know that the one-array solution is given by (3.1) and

$$\phi=\cosh(px-\omega t+\delta)+\sqrt{1-p^4/k_y^2}\cos(k_y y) \ ,$$

$$\omega=p^3+3k_y^2/p \ .$$

It is instructive to feed this into (3.1) and see how the array is produced. This will make understanding what follows easier (being able to "see" arrays in ϕ).

The solution (3.2) describes the collision between one such array with p_1,ω_1,k_y and another with p_2,ω_2,k_y. After collision both arrays retain their initial amplitudes, velocities, and spacings, but are phase shifted in x (and sometimes also in y as below).

The physical properties of the solution (3.1) and (3.2) can be seen to be determined by two parameters only. These are k_y/p_1^2 and p_2/p_1. The two-dimensional parameter space is divided into various regions in Fig. 3. Our solution is seen to include both situations in which arrays will shift by $\lambda/2$ in y ($s=-1$, broadly speaking if p_1 and p_2 are not too different) and also regions such that the phase shift in y does not occur ($s=1$, faster solitons

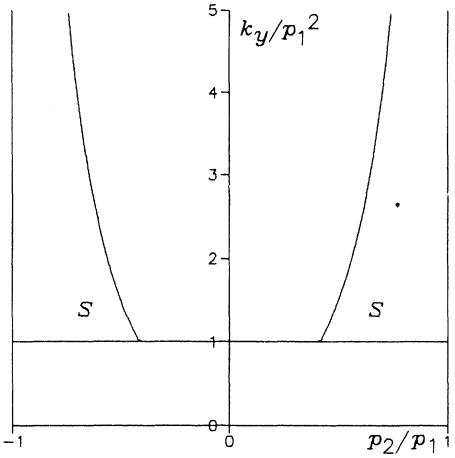

FIG. 3. Parameter space of two lump array collisions ($k_y/p_1^2>1$). Each point corresponds to one collision, due to the fact that p, ω, and k_y are the same before and after. Without loss of generality $|p_1|>|p_2|$. In the S regions the phase is shifted by $\lambda/2$ in y. Solutions along the curved part of the boundary of these regions are degenerate and correspond to one array of lumps but with $2k_y$. The k_y/p_1^2 axis (above one) corresponds to one lump array with k_y($k_y=0$ corresponds to two *line* soliton collisions).

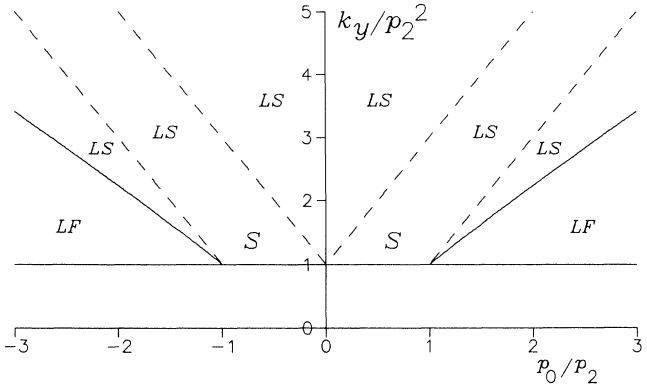

FIG. 4. Parameter space of lump array–line soliton collisions ($k_y/p_2^2>1$). In the S regions the phase of the lump array is shifted by $\lambda/2$ in y by the collision. LF corresponds to faster line soliton, LS to slower line soliton (as compared to lumps). Along the boundaries between LF and LS $\omega_0/p_0=\omega_2/p_2$ and the whole solution is stationary. Broken lines denote parameters corresponding to a plane soliton decaying to a smaller plane soliton and an array of lumps, not a collision: $b=0$, or $b=\pm\infty$ ($k_y=0$ corresponds to two *line* soliton collisions).

much larger than slower ones). Degenerate cases, such as $k_y=0$ (line solitons collide), or the solution reducing to just the one-lump soliton array, also appear following (3.2).

The dot in Fig. 3 is the result of an attempt at isolating the two-lump array collision of Fig. 2 and comparing it to an exact solution (the parameters of such an exact solution would fall roughly in the region of the dot). We see that agreement is good, as both here and in Fig. 2 amplitudes and spacings are preserved, and there is a $\lambda/2$ phase shift in y. (The ratios k_y/p_1^2 and p_1/p_2 can be checked with Fig. 2 by inspection.)

Finally, we will try to illustrate the line soliton–lump array collision mentioned in Sec. II but not illustrated there. After we had performed this calculation, an exact solution describing it was found formally [9]. It is, for ϕ (here a 3×3 determinant is calculated following Chap. 5 of Ref. [4]),

$$\phi=1+\exp[2(p_0x-\omega_0t)]+a\exp[2(p_1x-\omega_1t)]+ab^2\exp[-2(p_2x-\omega_2t)]$$
$$+2\cos(k_yy)\{\exp[(p_0+p_1)x-(\omega_0+\omega_1)t]+b\exp[-(p_2x-\omega_2t)]\}\ , \tag{3.3}$$

where

$$\omega_0=4p_0^3,\quad \omega_2=\frac{p_2^4+3k_y^2}{p_2},\quad \omega_1=\omega_0-\omega_2,\quad p_1=p_0-p_2\ ,$$

$$a=\frac{k_y^2}{k_y^2-p_2^4},\quad b=\frac{k_y^2-p_2^2(2p_0-p_2)^2}{k_y^2-p_2^2(2p_0+p_2)^2},\quad a\geq0\ .$$

Here a line soliton given by p_0 and ω_0 collides with an array of lumps characterized by p_2, ω_2, and k_y. The authors overlooked the y shift because they only considered $b\geq0$ (it occurs if and only if $b<0$). Figure 4 illustrates all regions and degenerate solutions in parameter space.

In both cases considered, shifts of arrays of lumps by $\lambda/2$ in y can occur when the difference in sizes between colliding solitons is not too great. This is intuitively acceptable, as conversely an enormous entity will always just "walk through" a tiny one. In contradistinction to the better known x shifts, those in y are "quantized" (either 0 or $\lambda/2$).

IV. OTHER INITIAL CONDITIONS

Up to now, our numerical simulations were chosen so that the phase was perturbed by a cosine function of varying amplitude δ. To show that the results obtained are in some sense generic, we now take a strongly localized perturbation such that the phase is

$$p(x-x_0)+\delta\exp(-ly^2)\ . \tag{4.1}$$

This initial condition will satisfy all constraints mentioned in Sec. II. The periodicity is taken to be the same as in previous simulations. The results for $\delta=0.016$ and $l=5$ are presented in Fig. 5. Note the essential similarity

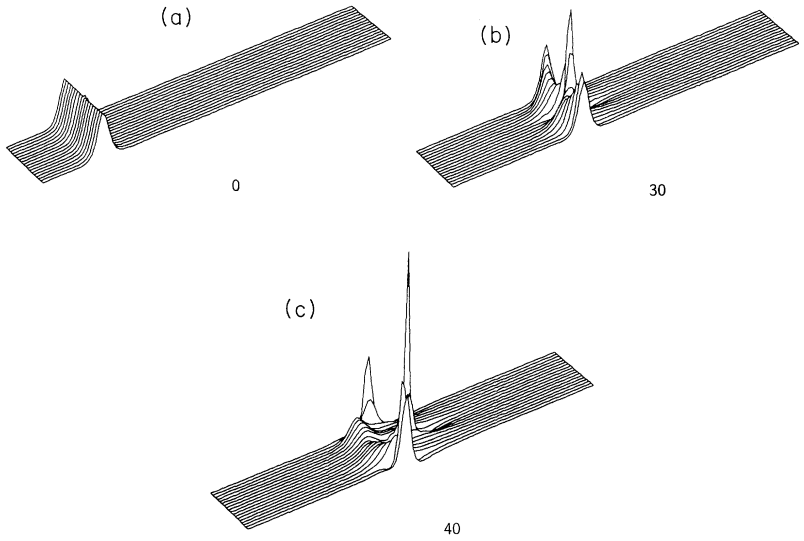

FIG. 5. Decay of a line soliton initially distorted by a strongly localized perturbation, $\delta=0.016$. Compare with Fig. 1 of Ref. [15].

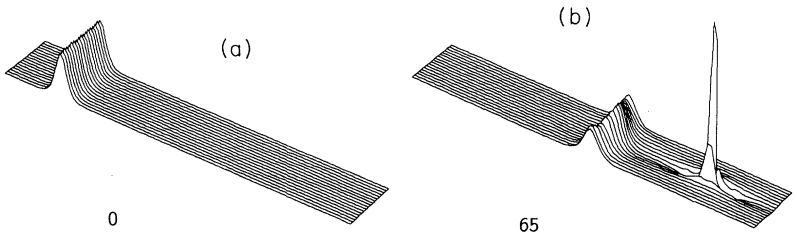

FIG. 6. Decay of a line soliton initially distorted by a perturbation that does not satisfy the constraints of the equation. Note how little this seems to matter on the time scale of the simulation. (This result is very similar to Fig. 1 of Ref. [15].) Here $\delta=0.016$.

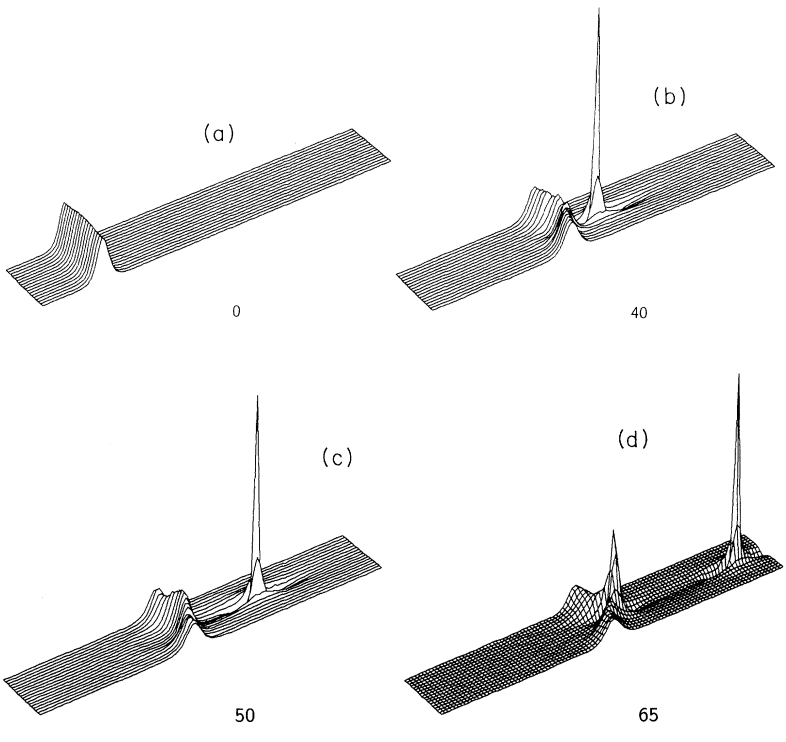

FIG. 7. Same as in Fig. 6, but for $\delta=0.04$. Compare with Fig. 1.

to Fig. 1 of Ref. [15] as far as production of large, two-dimensional lumps is concerned. However, due to the difference in initial condition, small "half period" lumps are additionally produced (these extra lumps were comparatively larger when $\delta=0.04$, not shown here).

Figures 6 and 7 present results for the improper initial conditions mentioned in Sec II, see (2.4). We took $\delta=0.016$ and 0.04, respectively. Nevertheless, the essential features of our previous, "correct" simulations are observed. This is in accord with the theory of Ref. [2]. Here δ is chosen to be identical with those of Ref. [15] and Fig. 1, respectively. In spite of the differences (modulation of amplitude rather than phase), the similarities are striking.

All in all, the simulations of Sec. II are indeed seen to be generic. This fact adds physical significance not only to them, but also to the exact solutions that abound in the literature.

ACKNOWLEDGMENTS

This work was partly supported by the Polish Committee for Scientific Research (KBN), Grant No. 2-2303-91-01.

APPENDIX: THE NUMERICAL ALGORITHM AND ITS STABILITY

We assume that Eq. (1.1) is defined for $x\in[-L_x,L_x]$ and $y\in[-L_y,L_y]$. The solution $n(x,y,t)$ is assumed to be well localized in x, so that we can put $[n_t+6nn_x+n_{xxx}]_{-L_x}=0$. With this assumption (1.1) is equivalent to

$$n_t+6nn_x+n_{xxx}+3\epsilon\int_{-L_x}^{x}n_{yy}dx'=0\ . \tag{A1}$$

Designating all variables in (A1) by the superscript zero and introducing the transformations

$$x^0=x/\nu_x-L_x,\quad y^0=y/\nu_y-L_y,\quad n^0=\beta n,\quad t^0=t/\gamma\ , \tag{A2}$$

where $\nu_x=\pi/L_x$ and $\nu_y=\pi/L_y$, we transform the original intervals of x and y into $[0,2\pi]$. Furthermore choosing

$$\beta=\nu_x^2/6,\quad \gamma=2\nu_x^3\ , \tag{A3}$$

we transform (A1) into

$$n_t+\tfrac{1}{2}\left[nn_x+n_{xxx}+\varepsilon A\int_0^x n_{yy}dx'\right]=0,\quad A=3\nu_y^2/\nu_x^4\ , \tag{A4}$$
$$x\in[0,2\pi],\quad y\in[0,2\pi]\ .$$

Equation (A4) was integrated by using the leapfrog time step:

$$n(t+\Delta t)-n(t-\Delta t)+\Delta t\left[nn_x+n_{xxx}+\epsilon A\int_0^x n_{yy}dx'\right]_{(t)}=0\ . \tag{A5}$$

This was combined with the pseudospectral method, as described e.g., in [21]. Thus the interval $[0,2\pi]$ for x is divided into $2N_x$ subintervals of length $\Delta x=\pi/N_x$, and similarly for y ($2N_y$ subintervals of length $\Delta y=\pi/N_y$). The function n, defined on the discrete mesh (x_j,y_l), $x_j=j\Delta x$, $y_l=l\Delta y$, can be transformed to discrete Fourier space for both x and y variables. Thus for each y_l we define the discrete Fourier transform in x:

$$\tilde{n}(k_x)=(2N_x)^{-1/2}\sum_{j=0}^{2N_x-1}n(x_j)\exp(-ik_xx_j)\ ,\qquad k_x=0,\pm1,\ldots,\pm N_x\ . \tag{A6}$$

The inverse transform is given by

$$n(x_j)=(2N_x)^{-1/2}\sum_{k_x}\tilde{n}(k_x)\exp(ik_xx)\Big|_{x=x_j}\ , \tag{A7}$$

where only one-half of the contributions at $k_x=\pm N_x$ are included in the sum over k_x. Replacing $x\to y$ and $j\to l$ everywhere in (A6) and (A7) we obtain the formulas for the discrete Fourier transform in y (for each x_j). The essence of the pseudospectral approach is to calculate the partial derivatives at the mesh points by differentiating the interpolation formula (A7) (or its analog in y) with respect to x (or y). Thus, for example,

$$n_x(x_j)=(2N_x)^{-1/2}\sum_{k_x}ik_x\tilde{n}(k_x)\exp(ik_xx_j)\ , \tag{A8}$$

etc. The integral in (A5) was calculated by using the Simpson formula, and the sums of the type of (A6) or (A8) were determined by using the well-known fast Fourier transform formalism as implemented in [22].

To examine the linear stability of the leapfrog time step (A5), we linearize Eqs. (A1) and (A5) by replacing $nn_x\to\alpha n_x$, where $\alpha=$const. Then we differentiate the linearized equation (A5) with respect to x, and look for the solution n in the form of a single Fourier harmonic in x and y, with the assumed exponential dependence on time:

$$n=\kappa^{t/\Delta t}\exp[i(k_xx+k_yy)]\ . \tag{A9}$$

Substitution of (A9) in (A5) (after linearization and differentiation $\partial/\partial x$) leads to a quadratic in κ:

$$\kappa^2-i2f(\Delta t,k_x,k_y,\alpha)\kappa-1=0\ ,\qquad f(\Delta t,k_x,k_y,\alpha)=\tfrac{1}{2}\Delta t(k_x^3-\alpha k_x-\varepsilon Ak_y^2/k_x)\ , \tag{A10}$$

where we have to assume $k_x\neq0$, see (A6). Numerical stability of the algorithm in question means that the solution (A9) cannot grow in time, i.e., $|\kappa|\le1$. In view of (A10) this is the case if and only if

$$|f(\Delta t,k_x,k_y,\alpha)|\le1\ . \tag{A11}$$

(α is assumed to be real.) Equation (A11) determines the maximum time step Δt for stability.

(i) $\varepsilon=-1$ *(KPI)*

$$|f| \leq \tfrac{1}{2}\Delta t[\,|k_x|(k_x^2+|\alpha|)+AN_y^2/|k_x|\,]\ . \tag{A12}$$

The right-hand side of (A12) as a function of $|k_x|$ has a single minimum, and therefore the maximum of this function for $|k_x|=1,\ldots,N_x$ is reached at $|k_x|$ either 1 or N_x. Assuming that $|\alpha|_{\max}(=|n|_{\max})$ is much less than either $AN_y^2(\gg 1)$ or N_x^2, the stability condition takes the form ($A=3\nu_y^2/\nu_x^4$, $\nu_x=\pi/L_x$, $\nu_y=\pi/L_y$, $N_x=\pi/\Delta x$, $N_y=\pi/\Delta y$)

$$\Delta t < \frac{2}{\max(\,AN_y^2, N_x^3+AN_y^2/N_x\,)}\ . \tag{A13}$$

(ii) $\epsilon=1$ *(KPII)*

Assuming again that $|\alpha|_{\max}$ is negligible, as above, the stability condition takes the form

$$\Delta t < \frac{2}{\max(\,AN_y^2, N_x^3\,)}\ . \tag{A14}$$

[1] B. B. Kadomtsev and V. I. Petviashvili, Dokl. Akad. Nauk SSSR **192**, 753 (1970) [Sov. Phys. Dokl. **15**, 539 (1970)].

[2] M. J. Ablowitz and J. Villarael, Stud. Appl. Math. **85**, 195 (1991).

[3] J. Satsuma, J. Phys. Soc. Jpn. **40**, 286 (1976); S. V. Manakov, V. E. Zakharov, L. A. Bordag, A. R. Its, and V. B. Matveev, Phys. Lett. **A63**, 205 (1977); K. A. Gorshkov, D. E. Pelinovskii, and Y. A. Stepanyants, Zh. Eksp. Teor. Fiz. **104**, 2704 (1993) [JETP **77**, 237 (1993)].

[4] E. Infeld and G. Rowlands, *Nonlinear Waves, Solitons and Chaos* (Cambridge University Press, Cambridge, 1992).

[5] A. S. Fokas and M. J. Ablowitz, J. Math. Phys. **25**, 2494 (1984).

[6] A. Arkadiev, A. Pogrebkov, and M. Palivanov, Physica **D36**, 189 (1989).

[7] A. A. Zaitsev, Dokl. Akad. Nauk SSSR **272**, 583 (1983) [Sov. Phys. Dokl. **28**, 720 (1983)].

[8] S. K. Zhdanov and B. A. Trubnikov, Pis'ma Zh. Eksp. Teor. Fiz. **39**, 110 (1984) [JETP Lett. **39**, 129 (1984)]; S. P. Burtsev, Zh. Eksp. Teor. Fiz. **88**, 1609 (1985) [Sov. Phys. JETP **61**, 959 (1985)]; J. Satsuma, J. Phys. Soc. Jpn. **40**, 286 (1976); Y. Kodama, Phys. Lett. A **129**, 223 (1988); M. Tajiri and Y. Murakami, J. Phys. Soc. Jpn. **58**, 3029 (1989); Y. Kodama and J. Gibbons, Phys. Lett. A **135**, 167 (1989).

[9] D. E. Pelinovskii and Y. A. Stepanyants, Zh. Eksp. Teor. Phys. **104**, 3387 (1993) [JETP **77**, 602 (1993)].

[10] S. V. Manakov, Physica D **3**, 420 (1981).

[11] A. S. Fokas and M. J. Ablowitz, Stud. Appl. Math. **69**, 211 (1983); X. Zhou, Commun. Math. Phys. **128**, 551 (1990).

[12] A. S. Fokas and L. Y. Sung, Inverse Prob. **8**, 673 (1992).

[13] V. Dryuma, Pis'ma Zh. Eksp. Teor. Fiz. **19**, 753 (1974) [JETP Lett. **19**, 381 (1974)].

[14] A. S. Fokas and V. Zakharov, J. Nonlinear Sci. **2**, 109 (1992).

[15] E. Infeld, A. Senatorski, and A. A. Skorupski, Phys. Rev. Lett. **72**, 1345 (1994).

[16] J. Weiss, M. Tabor, and G. Carnavale, J. Math. Phys. **24**, 522 (1983); R. Conte, A. P. Fordy, and A. Pickering, Physica D **69**, 33 (1993).

[17] V. E. Zakharov, Pis'ma Zh. Eksp. Teor. Fiz. **22**, 364 (1975) [JETP Lett. **22**, 174 (1975)]; E. Infeld and G. Rowlands, Proc. R. Soc. London Ser. A **366**, 537 (1979); E. A. Kuznetsov, M. D. Spector, and G. E. Fal'kovich, Physica D **10**, 379 (1984).

[18] P. Frycz and E. Infeld, Phys. Rev. A **41**, 3375 (1990).

[19] J. E. Lin and H. H. Chen, Phys. Lett. A **89**, 163 (1982).

[20] V. E. Zakharov, S. V. Manakov, S. P. Novikov, and L. P. Pitayevski, *Theory of Solitons* (Nauka, Moscow, 1980) [Plenum, New York, 1984].

[21] B. Fornberg and G. B. Whitham, Philos. Trans. R. Soc. London **289**, 373 (1978).

[22] C. Canuto, M. Y. Hussaini, A. Quarteroni, and T. A. Zang, *Spectral Methods in Fluid Mechanics* (Springer, Berlin, 1988).